Satellite monitoring of different vegetation types by differential optical absorption spectroscopy (DOAS) in the red spectral range

T. Wagner, S. Beirle, M. Grzegorski, U. Platt

Atmos. Chem. Phys. Discuss., 6, 7945–7958, 2006
www.atmos-chem-phys-discuss.net/6/7945/2006/

Atmospheric Chemistry and Physics Discussions

Satellite monitoring of different vegetation types by differential optical absorption spectroscopy (DOAS) in the red spectral range

T. Wagner, S. Beirle, M. Grzegorski, and U. Platt

Institut für Umweltphysik, University of Heidelberg, Heidelberg, Germany

Received: 29 May 2006 – Accepted: 11 August 2006 – Published: 16 August 2006

Correspondence to: T. Wagner (Thomas.wagner@iup.uni-heidelberg.de)

Abstract

A new method for the satellite remote sensing of different types of vegetation and ocean colour is presented. In contrast to existing algorithms, our method analyses weak narrow-band reflectance structures (i.e. "fingerprint" structures) of vegetation in the red spectral range. It is based on differential optical absorption spectroscopy (DOAS), which is usually applied for the analysis of atmospheric trace gas absorptions. Since the spectra of atmospheric absorption and vegetation reflectance are simultaneously included in the analysis, the effects of atmospheric scattering and absorption are automatically corrected. The inclusion of the vegetation spectra also significantly improves the results of the trace gas retrieval. The global maps of the fitting coefficients for the vegetation spectra (indicating the fraction of the observed ground scene covered by vegetation) illustrate the seasonal cycle of different vegetation types. In addition to the vegetation distribution on land, they also show patterns of biological activity in the oceans. Our results indicate that improved sets of vegetation spectra might lead to more accurate and more specific identification of vegetation type in the future.

1 Introduction

Vegetation has a strong influence on the cycles of trace gases and other important properties of the system earth, in particular the earth's energy budget. Vegetation modifies the ground albedo and thus has a strong impact on the amount of backscattered solar energy. Vegetation also strongly influences the water cycle through its influence on evaporation; the release of latent heat is important for the latitudinal energy distribution. Plants are also sources and/or sinks for many important trace gases, in particular greenhouse gases. Therefore, the precise knowledge of the spatio-temporal variation of the biological activity is an important prerequisite for the correct understanding and simulation of global trace gas budgets and of the earth's climate. Of special importance is the monitoring of the human-induced change of the global vegetation patterns,

ACPD

6, 7945–7958, 2006

e.g. caused by biomass burning or climate change.

Algorithms for the remote sensing of vegetation have been developed and are successfully applied to satellite observations for a long time. Typically they are based on the measured radiance in the red and near-infrared part of the spectrum. Over this wavelength range, the reflectivity of vegetation changes strongly (Fig. 1), caused by the absorption of various kinds of chlorophyll and pigments. Thus a clear vegetation signal can be easily derived. Definitions of various kinds of vegetation indices can be found in Birth and McVey (1968), Jordan (1969), Rouse et al. (1973), Huete (1988), Gutman (1991), and Jensen (2000).

Here we present a new vegetation algorithm which can be applied to new satellite sensors with moderate spectral resolution (but only coarse spatial resolution). A similar method was already applied to airborne measurements by Clark et al. (1995). In contrast to the existing algorithms, our method exploits the narrow-band spectral information of the vegetation reflectance, which allows in particular to discriminate different types of vegetation. One additional advantage is that the influence of atmospheric scattering and absorption is automatically corrected.

2 The instrument: GOME on ERS-2

The Global Ozone Monitoring Experiment (GOME) is one of several instruments aboard the European research satellite ERS-2 (European Space Agency (ESA), 1995; Burrows et al., 1999). It consists of a set of four spectrometers that simultaneously measure sunlight reflected from the Earth's atmosphere and surface in 4096 spectral channels covering the wavelength range between 240 and 790 nm with moderate spectral resolution (FWHM: 0.2–0.4 nm). The satellite operates in a nearly polar, sun-synchronous orbit at an altitude of 780 km with an equator crossing time of approximately 10:30 a.m. local time. While the satellite orbits in an almost north-south direction, GOME scans the surface of earth in the perpendicular east-west direction. During one scan, three individual ground pixels are observed, each covering an area of 320 km east to west by 40 km north to south. They lie side by side: a west, a centre, and an east pixel. The Earth's surface is entirely covered within 3 days, and poleward from about 70° latitude within 1 day.

3 Data analysis

We retrieve information on vegetation and atmospheric absorbers using Differential Optical Absorption Spectroscopy (DOAS, see Platt, 1994). The DOAS method applies a high-pass filtering to the measured spectra of scattered sun light (from various platforms) and thus enables the detection of several weak atmospheric absorbers. Our DOAS analysis is performed in the wavelength interval 605–683 nm. It is based on the algorithm developed for the analysis of the atmospheric absorptions of water vapour and the oxygen molecule (O_2) and dimer (O_4) as described in detail in Wagner et al. (2004, 2005). Using this algorithm, however, it turned out that over the continents often strong spectral structures appeared in the measured spectra, which could not be accounted for by the atmospheric absorptions of O_2, O_4, and H_2O. These spectral structures showed up in the residual of the DOAS analysis causing strong systematic errors of the trace gas retrievals. In some cases, even apparent negative trace gas absorptions were found (Fig. 1).

After various possible instrumental and methodological reasons for this structure were investigated and could be excluded, we studied whether spectral structures caused by the albedo of specific surface types might be responsible for the observed spectral residuals. Since the problems occurred only over areas with vital vegetation, we took a closer look at the spectral albedos of different kinds of vegetation (vegetation reflectance spectra reproduced from the ASTER Spectral Library through the courtesy of the Jet Propulsion Laboratory, California Institute of Technology, Pasadena, California, see also http://speclib.jpl.nasa.gov/).

It soon turned out that the residual spectral structures were similar to the high-pass-filtered reflectance spectra measured over vegetation (Fig. 2). Moreover, if the vege-

ACPD
6, 7945–7958, 2006

EGU

tation spectra were included in the spectral analysis, the residual structures and the errors for the retrieval of the atmospheric absorbers were strongly reduced (Fig. 1). It is interesting to note that in the red spectral range not only the absolute values of the albedo, but also the narrow-band spectral structures (for the spectral resolution of about 8 nm, see http://speclib.jpl.nasa.gov/) are very weak (<1%). For the corresponding weak variations of the observed radiance, it is thus possible to include the vegetation spectra directly in the DOAS fitting procedure (like the trace gas reference spectra). One particular advantage of the simultaneous fitting of atmospheric trace gas absorptions and spectral albedo structures is that the correction of atmospheric scattering and absorption processes that is necessary for conventional algorithms is automatically included in the retrieval of the vegetation results. Since the used vegetation spectra were obtained for the complete field of view of the instrument covered by vegetation, we expect coefficients for the vegetation spectra derived by the spectral fitting procedure to range between zero (for no vegetation in the field of view of the satellite instrument) to unity (for a ground pixel completely covered by vegetation). The retrieved fitting coefficients can thus be interpreted as fraction of the observed ground pixel covered by vegetation. However, it turned out that the fitting coefficients for the different kinds of vegetation are often much larger than the expected maximum value of unity. In addition, we found that even with the inclusion of the vegetation spectra, still systematic spectral structures in the residual remained (Fig. 1). These findings might indicate that the used vegetation spectra are not perfectly suited for the kind of spectral analysis we perform for the satellite spectra (of course they have been recorded for other purposes). Several reasons (or their combination) might be responsible for these observed issues. First, the spectral resolution of the vegetation spectra is much coarser than the spectral resolution of the GOME instrument (FWHM about 8 nm compared to about 0.4 nm). To study this potential error source, we mathematically reduced the spectral resolution of the GOME measurements and of the trace gas reference spectra before the fitting process. For that purpose we convoluted them by Gaussian functions of different widths (full width at half maximum either 4 nm or 8 nm). Using these modified spectra, the absolute values of the retrieved results for the different vegetation types became systematically smaller. However, the residual structure did not substantially change. Thus, it is probable that the coarse resolution of the vegetation spectra is not the sole reason for the remaining residual structures. Another possible reason might be that the spectral calibration of the vegetation spectra is not very accurate (within about a few nm, see http://speclib.jpl.nasa.gov/). However, if we allowed spectral shifting of the vegetation spectra during the fitting procedure, the results did not change substantially.

In addition, the residual structures might be caused by the fact that the selected vegetation spectra are not fully representative for the measured spectral structures of vegetation. Indications for this possibility are also found from the comparison of the fitting coefficients for the different vegetation types (see below). Especially, the observed interferences between the different vegetation types and also with the ocean colour indicate that the used vegetation spectra did not perfectly fit to the observed spectral structures. We also found that the results are sensitive to variations of the selected wavelength range. Differences between the vegetation spectra and the satellite observations might be also partly caused by the fact that both observations were performed with a different field of view and under different angles of observation and solar illumination.

4 Results

In Fig. 3, monthly mean maps for the results of the different vegetation spectra are shown for two selected months (March and September 1998). Four types of vegetation (conifers, deciduous trees, grass and dry grass) were included in the spectral fitting procedure (spectra reproduced from the ASTER Spectral Library through the courtesy of the Jet Propulsion Laboratory, California Institute of Technology, Pasadena, California, see also http://speclib.jpl.nasa.gov/).

Only measurements with an O_2 absorption >80% of the maximum O_2 absorption

ACPD

6, 7945–7958, 2006

Satellite monitoring of vegetation by DOAS

T. Wagner et al.

EGU

were selected to exclude mainly cloudy skies (for details of the cloud-selection algorithm, see Wagner et al., 2005 and 2006). While for dry grass the results were close to zero above the whole globe, (not shown), the results for the three other vegetation spectra showed characteristic spatio-temporal patterns. The relative patterns for deciduous trees and grass are almost identical. This is an interesting finding, since both spectra show different narrow-band spectral structures (Fig. 2). It indicates that the observed spectral structures of vegetation contain components of both vegetation spectra. For conifers, different patterns were found. Enhanced values are mainly located over the mid and high-latitude regions of the northern hemispheric continents, in good agreement with the global distribution of cool coniferous forest.

It is interesting to note that especially the results for conifers are also influenced by the ocean colour. Enhanced fitting coefficients for the conifer spectrum are found over regions with high biological activity, particularly close to the mouths of big rivers (see Fig. 4). Of course, this should naturally not be expected. At the moment we can only speculate that parts of the spectral signatures of ocean colour (e.g. chlorophyll and additional pigments) are very similar to those of the vegetation spectrum for conifers. In some of these regions, also corral reefs exist, which might have also contributed to the measured vegetation signal. Future work should aim to understand this effect in more detail. With an improved set of spectra for different kinds of land vegetation and ocean colours, it will hopefully become possible to separate the effects of ocean colour and conifers by their spectral signatures. However, using the currently available spectra this was not possible (for possible reasons, see the discussion at the end of Sect. 3).

From our satellite results of vegetation and ocean colour the seasonal cycle of the biological activity in different parts of the world can be clearly followed and similar patterns are found in different years. The vegetation results can in principle be retrieved on a daily basis; averaging over longer periods of time leads to more consistent patterns, mainly because then the masking due to clouds has a much weaker impact.

5 Discussion and conclusions

We included spectra of the spectral reflectance for different types of vegetation in the DOAS fitting procedure for the analysis of atmospheric trace gases in the red part of the spectrum. Besides a significant improvement of the fitting results for the atmospheric trace gases, this inclusion enables also the retrieval of vegetation properties from satellite observations. In contrast to the analysis of vegetation indices in the red and near-infrared part of the spectrum (e.g. Jensen, 2000), here we made use of the narrow-band spectral information. In the red part of the spectrum the amplitude of the spectral structures of vegetation is small (<1%), but can be clearly identified in the measured spectra. It is in particular possible to identify different kinds of vegetation. The results of our analysis are expressed as fitting coefficients for the different vegetation spectra, which can be interpreted as fraction of the observed ground pixel covered by vegetation.

Our new method is not only sensitive to vegetation over the continents, but also to the biological activity in the oceans. Especially in the mouths of big rivers and over areas with coral reefs strong vegetation signals can be found. One particular advantage of our new vegetation algorithm is that the correction of atmospheric scattering and absorption processes is automatically included in the retrieval of the vegetation results.

Our results indicate that the currently available vegetation spectra are not of sufficient quality to obtain optimum DOAS fitting results, which is understandable since these spectra were of course taken for other purposes. Especially the spectral resolution and the spectral calibration should be improved. In addition, it seems that the selected spectra might not be fully representative for the spectral structures typically observed by satellite sensors. We therefore strongly recommend the measurement of new vegetation spectra covering a larger variety of species including marine algae with better spectral quality. Our results indicate that using this new method it might be possible in the future to monitor the seasonal cycles of different types of vegetation on a global scale.

Our new vegetation algorithm can also be applied to additional satellite sensors with sufficient coverage of the red spectral region, namely the SCanning Imaging Absorption SpectroMeter for Atmospheric ChartographY (SCIAMACHY) on ENVISAT in Bovensmann et al. (1999) SCIAMACHY and the three instruments of the GOME-II series ([EUMETSAT, 2005). Compared to the GOME-I instrument, the spatial resolution of these sensors is much better (footprints of 30×60 km^2 and 40×80 km^2, respectively) allowing to retrieve much finer details of the vegetation patterns.

Acknowledgements. The spectra of the vegetation reflectance were reproduced from the ASTER Spectral Library through the courtesy of the Jet Propulsion Laboratory, California Institute of Technology, Pasadena, California. ©1999, California Institute of Technology. ALL RIGHTS RESERVED, see also http://speclib.jpl.nasa.gov/. Special thanks are expressed to M. Bugert for helpful information on chlorophyll spectra.

References

Birth, G. S. and McVey, G.: Measuring the color growing turf with a reflectance spectrophotometer, Agronomy J., 60, 640–643, 1968.

Bovensmann, H., Burrows, J. P., Buchwitz, M., Frerik, J., Noël, S., Rozanov, V. V., Chance, K. V., and Goede, A.: SCIAMACHY - mission objectives and measurement modes, J. Atmos. Sci., 56, 127–150, 1999.

Burrows, J. P., Weber, M., Buchwitz, M., Rozanov, V., Ladstätter-Weißenmayer, A., Richter, A., DeBeek, R., Hoogen, R., Bramstedt, K., Eichmann, K. -U., Eisinger, M., and D. Perner: The Global Ozone Monitoring Experiment (GOME): Mission Concept and First Scientific Results, J. Atmos. Sci., 56, 151–175, 1999.

Clark, R. N., King, T. V. V., Ager, C., and Swayze, G. A.: Initial vegetation species and senescence/stress mapping in the San Luis Calley, Colorado using imaging spectrometer data. Proceedings: Summitville Forum '95, edited by: Posey, H. H., Pendelton, J. A., and Van Zyl, D., Colorado Geological Survey Special Publication, 38, 64–69, 1995.

ESA Publication Division (SP-1182), GOME, Global Ozone Monitoring Experiment, users manual, edited by: Bednarz, F., European Space Research and Technology Centre (ESTEC), Frascati, Italy, 1995.

EUMETSAT, GOME-2 Products Guide, available at http://www.eumetsat.int, 2005

Gutman, G.: Vegetation indices from AVHRR: An update and future prospects, Remote Sens. Environ., 35, 121–136, 1991.

Huete, A. R.: A Soil-Adjusted Vegetation Index (SAVI), Remote Sensing of Environment, 25, 295–309, 1988.

Jensen J. R.: Remote Sensing of the Environment: An Earth Resource Respective, Prentice Hall, Upper Saddle River, New Jersey, pp 353, 2000.

Jordan, C. F.: Derivation of leaf-area index from quality of light on the forest floor, Ecology, 50(4), 663–666, 1969.

Platt U.: Differential optical absorption spectroscopy (DOAS), Air monitoring by spectroscopic techniques, M.W. Sigrist, Ed., Chemical Analysis Series, 127, John Wiley & Sons, Inc, 1994.

Rouse, J. W., Haas, R. H., Schell, J. A., and Deering, D. W.: Monitoring Vegetation Systems in the Great Plains with ERTS, Proceedings, Third Earth Resources Technology Satellite-1 Symposium, Greenbelt: NASA SP-351, 309–317, 1974.

Wagner, T., Beirle, S., Grzegorski, M., Sanghavi, S., and Platt, U.: El-Niño induced anomalies in global data sets of water vapour and cloud cover derived from GOME on ERS-2, J. Geophys. Res, 110, D15104, doi:10.1029/2005JD005972, 2005.

Wagner, T., Beirle, S., Grzegorski, M., and Platt, U.: Global trends (1996 to 2003) of total column precipitable water observed by GOME on ERS-2 and their relation to surface-near temperature, J. Geophys. Res., 111, D12102, doi:10.1029/2005JD006523, 2006.

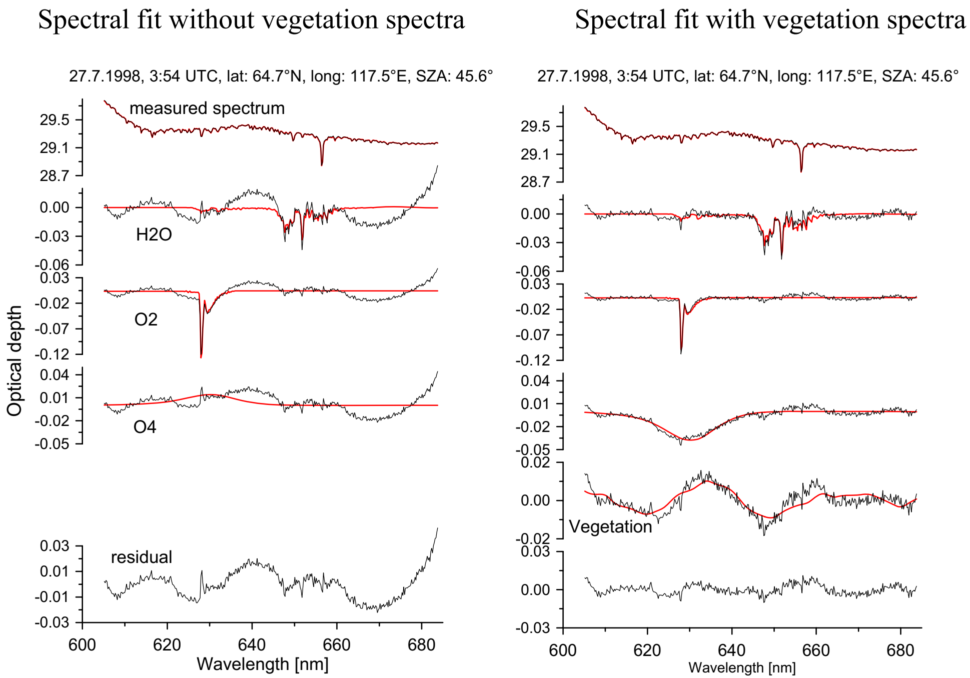

Fig. 1. Results of a spectral DOAS analysis of water vapor and the oxygen molecule (O_2) and dimer (O_4) without (left) and with (right) inclusion of vegetation reflectance spectra. For measurements over vital vegetation strong and systematic spectral residuals appear, if the reflectance spectra of vegetation are not included.

ACPD

6, 7945–7958, 2006

Satellite monitoring of vegetation by DOAS

T. Wagner et al.

EGU

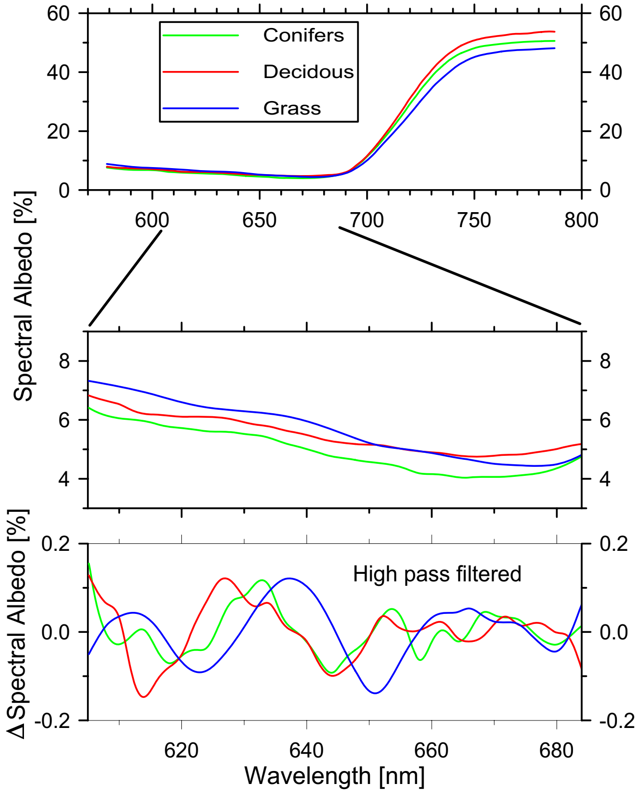

Fig. 2. Top: Spectra of the reflectance over different kinds of vegetation, reproduced from the ASTER Spectral Library through the courtesy of the Jet Propulsion Laboratory, California Institute of Technology, Pasadena, California. The strong change of the reflectance between the red and infrared part of the spectrum is usually exploited for the remote sensing of vegetation. In the red part of the spectrum the reflectance is small (middle), but contains characteristic spectral structures (displayed after high-pass filtering, bottom).

ACPD
6, 7945–7958, 2006

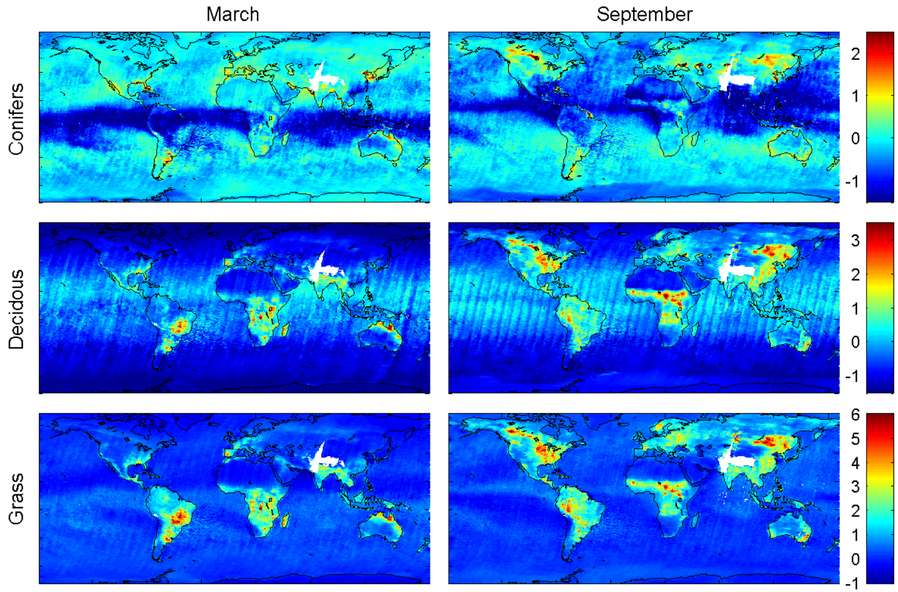

Fig. 3. Global maps of the monthly mean results of the DOAS retrieved fitting coefficients for different vegetation spectra. The results for deciduous trees and grass are very similar; those for conifers show different spatial patterns. The effect of the seasonal cycle is clearly visible.

ACPD

6, 7945–7958, 2006

Satellite monitoring of vegetation by DOAS

T. Wagner et al.

EGU

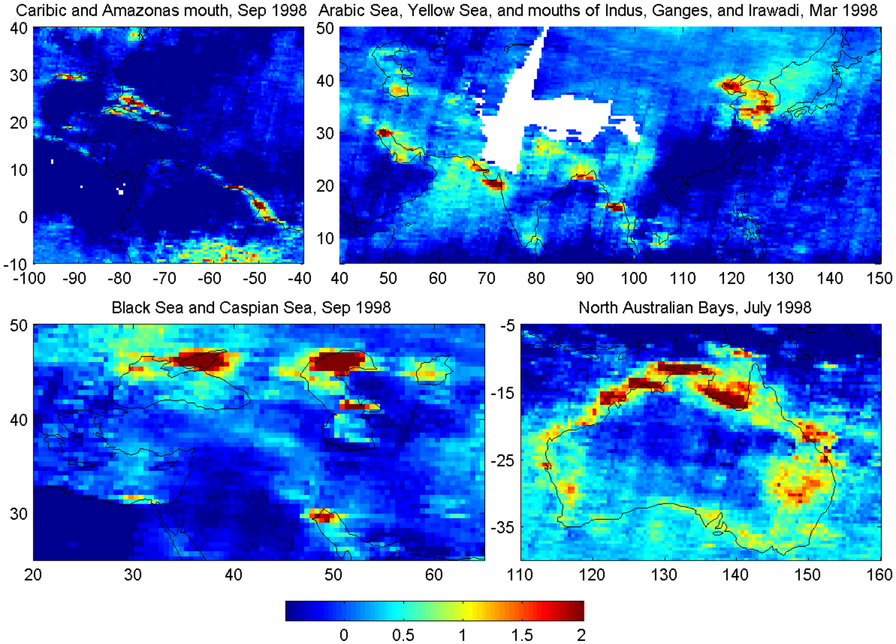

Fig. 4. The retrieved fitting coefficients for the conifer spectra are also strongly influenced by the ocean colour. Over areas with strong biological activity, high values are found.

ACPD
6, 7945–7958, 2006

Satellite monitoring of vegetation by DOAS

T. Wagner et al.

EGU